Electronic Supplementary Material (ESI) for RSC Advances.

Synthesis, mechanism and efficient modulation of fluorescence dye by photochromic pyrazolone with energy transfer in crystalline state

Yinhua Li, Jixi Guo,* Anjie Liu, Dianzeng Jia,* Xueyan Wu, and Yi Chen

Key laboratory of energy materials chemistry, ministry of education; Key laboratory of advanced functional materials, autonomous region; Institute of Applied Chemistry, Xinjiang University, Urumqi 830046, Xinjiang, P. R. China

Corresponding author: Tel.: +86-991-8583083; Fax: +86-991-8588883;
E-mail address:jxguo1012@163.com; jdz0991@gmail.com

Table of Contents

Molecular structure characterization data

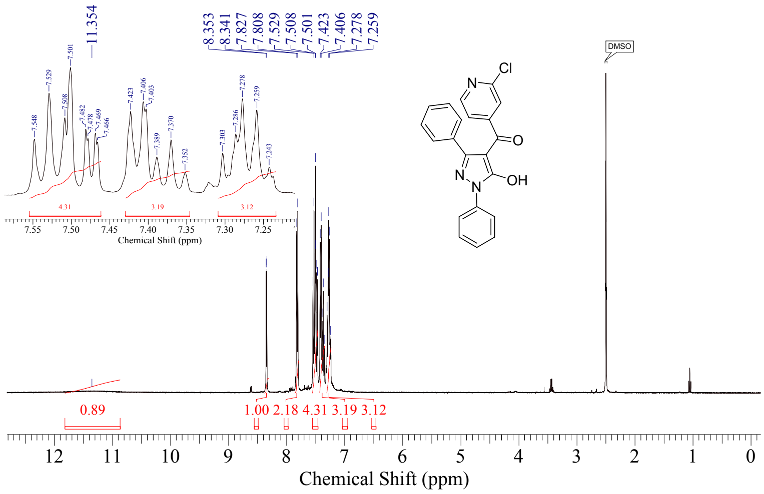

Figure S1. ^{1}H NMR of **DP3Cl4PyBP** (400 MHz, DMSO-d_6).

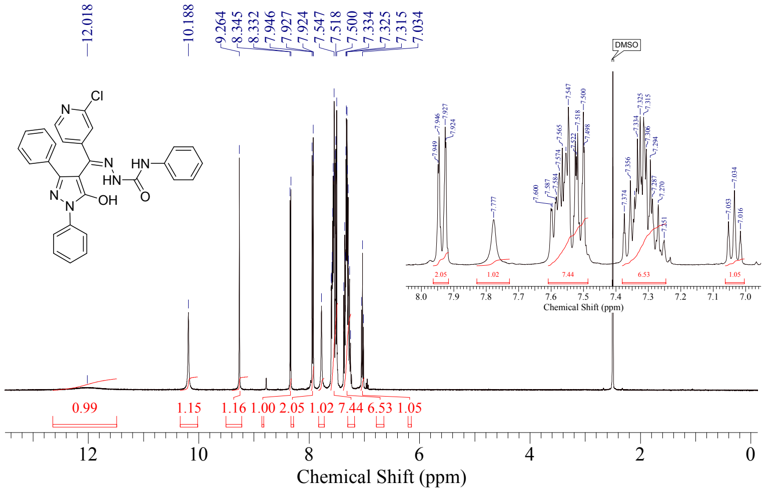

Figure S2. ^{1}H NMR of **1** (400 MHz, DMSO-d_6) .

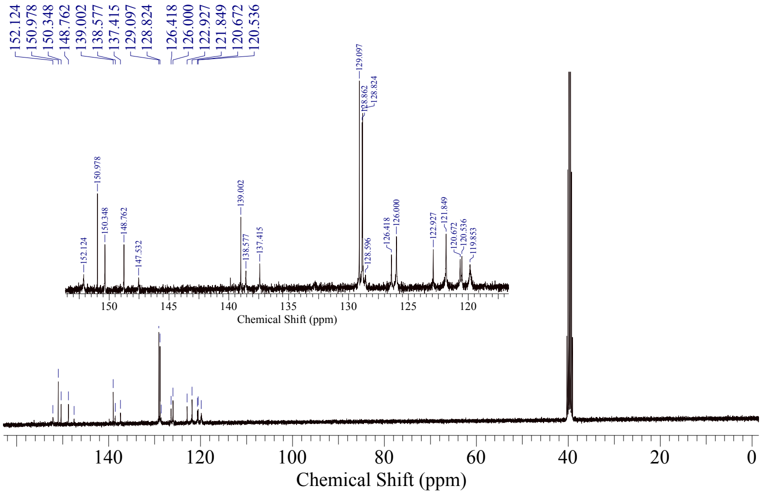

Figure S3. ^{13}C NMR of **1** (120 MHz, DMSO-d_6).

Kinetics plot of compound 1

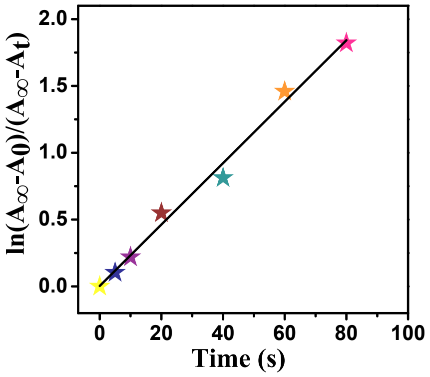

Figure S4. First-order kinetics plot of photocolouration reaction of photochromic **1** at 431 nm under the 365 nm light irradiation.

The crystal structure and data of 1

Table S1. Crystal data and structure refinement for **1**

	1
Empirical formula	$C_{31}H_{31}ClN_6O_4$
Formula weight	587.07
Temperature	298(2) K
Wavelength	0.71073 Å
Crystal system	Triclinic
space group	$P\bar{1}$
Unit cell dimensions	a = 11.500(6) Å α = 69.738(8) deg.
	b = 12.190(7) Å β = 70.732(8) deg.
	c = 12.237(6) Å γ = 70.189(8) deg.
Volume	1469.5(13) $Å^3$
Z, Calculated density	2, 1.327 Mg/m^3
Absorption coefficient	0.177 mm^{-1}
F(000)	616
Crystal size	0.50 x 0.30 x 0.20 mm
Theta range for data collection	2.28 to 24.99
Limiting indices	-11<=h<=13, -13<=k<=14, -11<=l<=14
Reflections collected / unique	7540 / 5082 [R(int) = 0.0330]
Completeness to theta = 24.99	98.2 %

Absorption correction	None
Max. and min. transmission	0.9654 and 0.9167
Refinement method	Full-matrix least-squares on F^2
Data / restraints / parameters	5082 / 6 / 394
Goodness-of-fit on F^2	1.006
Final R indices [I>2sigma(I)]	R_1 = 0.0664, wR_2 = 0.1723
R indices (all data)	R_1 = 0.1255, wR_2 = 0.2084
Extinction coefficient	0.0036(19)
Largest diff. peak and hole	0.249 and -0.275 e.Å^{-3}

Table S2. Selected bond lengths (Å) for **1**

1			
O(1)-C(7)	1.325(4)	N(2)-C(9)	1.340(4)
O(1)-H(10)	0.8201(11)	N(3)-C(16)	1.296(4)
O(2)-C(22)	1.225(4)	N(3)-N(4)	1.362(4)
O(3)-C(29)	1.415(8)	N(4)-C(22)	1.372(5)
O(3)-H(30)	0.8200	N(4)-H(4N)	0.863(10)
O(4)-C(31)	1.555(9)	N(5)-C(22)	1.346(5)
O(4)-H(40)	0.8200	N(5)-C(23)	1.421(5)
N(1)-N(2)	1.356(4)	N(5)-H(5N)	0.854(10)
N(1)-C(7)	1.372(4)	N(6)-C(19)	1.312(5)
N(1)-C(6)	1.440(4)	N(6)-C(20)	1.340(5)

Table S3. Hydrogen bonds for **1**

D-H...A	**d(D-H) (Å)**	**d(H...A) (Å)**	**d(D...A) (Å)**	**∠(DHA) (°)**
O(1)-H(10)...O(2)#1	0.8201(11)	1.80(3)	2.542(4)	149(7)
O(3)-H(30)...O(4)	0.82	1.90	2.702(6)	167.2
O(4)-H(40)...N(6)	0.82	2.09	2.904(6)	171.5
N(4)-H(4N)...O(3)#2	0.863(10)	2.24(2)	2.992(5)	146(3)
N(5)-H(5N)...O(3)#2	0.854(10)	2.051(16)	2.864(6)	159(3)

Symmetry codes: #1 -x+2,-y+1,-z+1 #2 x+1,y,z-1

The volume optimization of reprecipitates 1

The stock solution of compound **1** (2.5 mM) in ethanol was prepared. The examination of PL spectrum indicated that the emission intensity demonstrates weak change in lower volume ratio (<1.5). While the emission intensity sharply increases in emission maximum (λ_{em} = 465), when volume ratios were changed from 1.5 to 2. In the mixture with “higher” volume ration (>2), the intensity of PL maintaines stable (Figure S5). So, reprecipitates **1** was prepared in mixed solvent with 67% volume fraction. With the continuation of aging time for 1h, 2h, 5h and 10h, the morphology of reprecipites **1** vary from 0D nanoballs to 1D nanorods. The nanoballs are cohered, fused, rearranged and finally created the fully 1D nanorods as showe in figure S6. The driving force of growing is related to the decreasing of curvature strain and membrane defects, which can reduce the curvature energy and defects, and improve the stability for nanoballs.[1,2] The ethanol is an inevitable factor for fusion to provide the mobility for molecules. The bulk samples of reprecipites **1** showe size-dependent photochromic properties. The yellow nanoballs do not undergone photochromic reaction, while the white nanorods exhibit the photochromic reactions similarly with that of crystalline-state compound **1** (Figure S7). The distinction of properties is ascribed to morphologies, which is crucial for **1** to achieve fluorescence modulation in aggregated state.

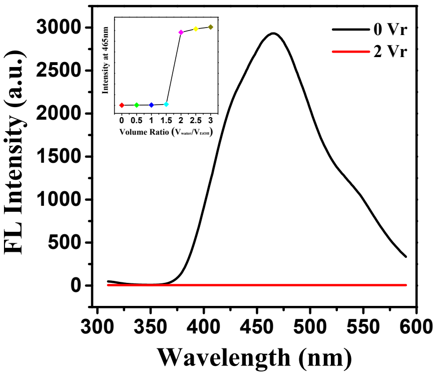

Figure S5. The fluorescence spectra of **1** in ethanol and in water-ethanol mixed solution with volume ratio 0 and 2. The insert: emission intensity of **1** at 465 nm with different volume ratio.

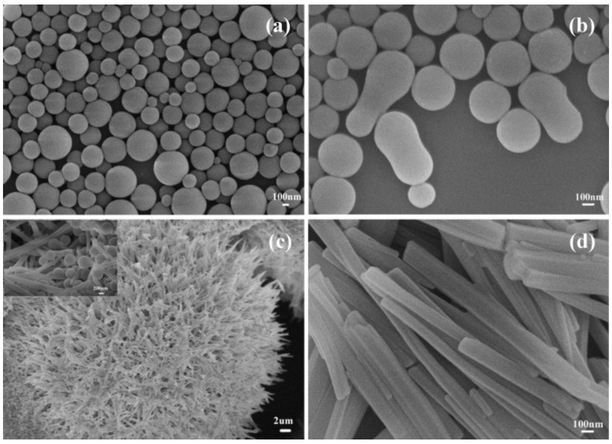

Figure S6. The SEM images of **1** aging for 1 h (a), 2 h (b), 5 h (c) and 10 h (d) in 67% water-ethanol mixed solution.

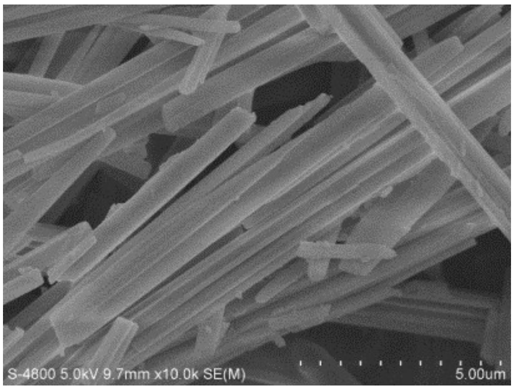

Figure S7. SEM spectra of crystalline state **1**.

The isomers of *K*-form

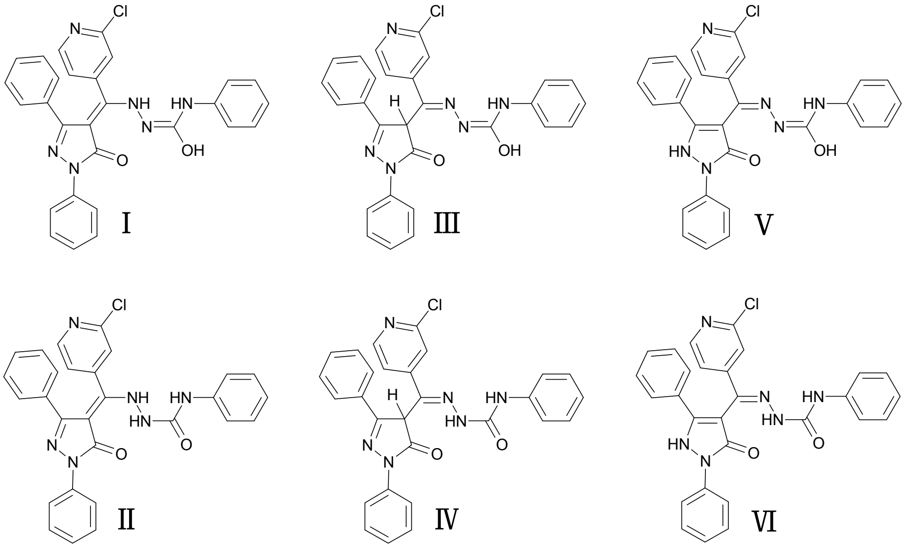

Figure S8. The six isomers of *K*-form.

The calculated UV-Vis analysis

Table S4. Selected theoretical UV spectral characteristics of six isomers.

Compound	Excited state	Excitation energy (eV)	λ_{abs} (nm)	*f*	MO composition	
I	S1	2.2696	546.28	f=0.0070	H-0→L+0	(99%)
	S2	2.7400	452.50	f=0.0964	H-1→L+0	(98%)
	S3	3.0769	402.96	f=0.0593	H-2→L+0	(94%)
	S4	3.4851	355.76	f=0.0012	H-4→L+0	(12%)

					H-**3**→L+0	(94%)
II	S1	2.5642	483.53	f=0.0088	H-0→L+0	(99%)
	S2	3.0765	403.00	f=0.2314	H-1→L+0	(98%)
	S3	3.5053	353.70	f=0.0627	H-2→L+0	(96%)
	S4	3.7298	332.42	f=0.0046	H-4→L+0 H-3→L+0	(23%) (74%)
III	S1	3.1801	389.88	f=0.0063	H-0→L+0	(96%)
	S2	3.5253	351.70	f=0.6317	H-1→L+0	(88%)
	S3	3.5570	348.56	f=0.1446	H-1→L+1	(52%)
	S4	3.6280	341.74	f=0.1575	H-1→L+1 H-0→L+1	(50%) (45%)
IV	S1	3.2260	384.33	f=0.0024	H-0→L+0	(95%)
	S2	3.1135	360.05	f=0.2087	H-1→L+0	(98%)
	S3	3.7492	330.70	f=0.2402	H-2→L+0 H-0→L+1	(11%) (85%)
	S4	3.7819	327.83	f=0.0353	H-3→L+0	(78%)
V	S1	3.1916	388.47	f=0.4380	H-0→L+0	(87%)
	S2	3.3685	368.07	f=0.0329	H-1→L+0	(89%)
	S3	3.4584	356.49	f=0.1488	H-0→L+1	(79%)
VI	S1	2.9618	418.61	f=0.1030	H-0→L+0	(97%)
	S2	3.4702	357.28	f=0.0133	H-1→L+0	(86%)
	S3	3.6469	339.97	f=0.3148	H-0→L+1	(87%)

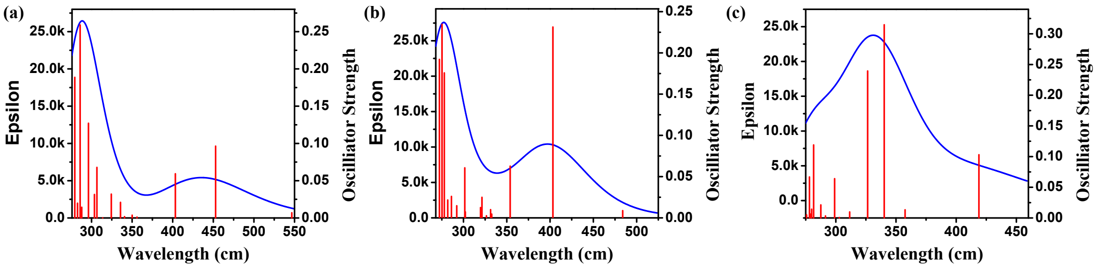

Figure S9. The theoretical absorption spectra with oscillator (a) I, (b) II, (c) VI.

The SEM spectra of reprecipites DPA

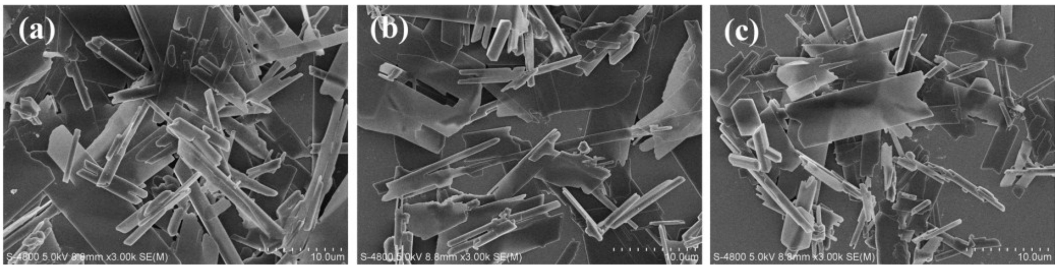

Figure S10. SEM spectra of reprecipites **DPA** for aging 1 h (a), 5 h (b), 10 h (c) in 67% water-ethanol mixed solution.

Fluorescence decay curves for TCCM

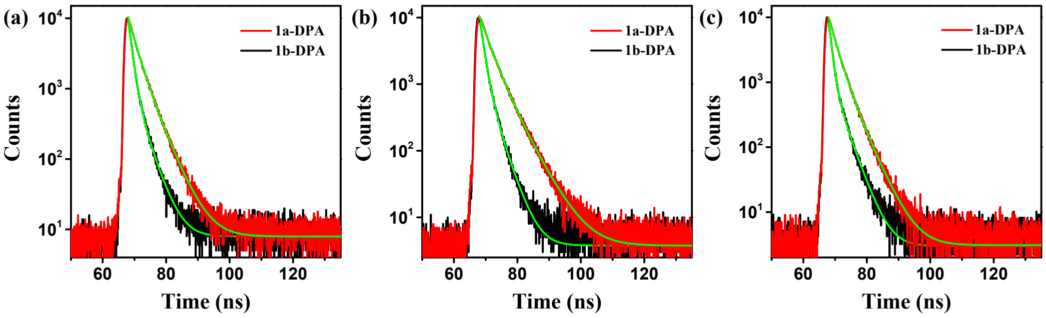

Figure S11. Emission decay profiles of different **TCCM** (a) 5%, (b) 15%, (c) 20%.

Table S5. The fluorescence modulation ratios, fitting average lifetimes and intermolecular energy transfer efficiency for **1** and **TCCM** materials before and after irradiation.

Compound	FM Ratio	Before irradiation	After irradiation	E_T
		τ_{on}(ns)	τ_{off} (ns)	
1	-	1.89	1.87	-
5%	28%	3.20	1.77	45%
10%	21%	3.79	1.70	55%
15%	29%	3.76	1.84	51%
20%	31%	3.0	1.84	41%

Reference

1. H. B. Fu and J. N. Yao, *J. Am. Chem. Soc.*, 2001, **123**, 1434-1439.
2. D. M. Vriezema, J. Hoogboom, K. Velonia, K. Takazawa, P. C. M. Christianen, J. C. Maan, A. E. Rowan and R. J. M. Nolte, *Angew. Chem. Int. Ed.*, 2003, **42**, 772-776.